

Microstructure Evolution in Ti-Ta Bilayer Films on Si(001) and Poly-Si Studied by Time-Resolved X-ray Diffraction, Light Scattering and Resistance Analysis

A.S. Özcan¹, K.F. Ludwig, Jr.¹, K.P. Rodbell², C. Lavoie², C. Cabral, Jr.²,
J.M.E. Harper², and J.L. Jordan-Sweet²

¹Boston University, Physics Department, Boston, MA

²IBM T.J. Watson Research Center, Yorktown Heights, NY

Metal silicides have been extensively studied due to their use in the microelectronics industry^{1,2,3}. Titanium disilicide has been used widely in Si ultra-large-scale integration (ULSI) technology because of its low resistivity and relatively high thermal stability. TiSi₂ exists in two polymorphs, with crystallographic designations C49 and C54. The C54 phase has a significantly lower resistivity (15-20 μΩ-cm) than does the C49 structure (60-75 μΩ-cm). Although the technologically desired C54 phase is the equilibrium phase of the disilicide, under most conditions the C49 phase is kinetically favored. The transformation to the C54 phase can be difficult, particularly in submicron features. Interposing a thin layer of a refractory metal, such as Mo or Ta, is one method for enhancing the C54 phase formation^{4,5,6}. Two major mechanisms have been suggested and explored to explain this enhancement^{7,8,9}. The first is the creation of a template layer associated with the ternary C40 silicide phase or a metal-rich phase. The structure of the C40 phase is closely related to that of the C54 phase, and, if it forms first, it can act as a template on which the C54 phase can nucleate. The second mechanism, grain size effect, suggests that the addition of a refractory metal could decrease the average C49 grain size, thus creating more triple-junction grain boundaries where the C54 phase can nucleate. The true mechanism still needs to be confirmed since there are arguments for and against both suggested mechanisms.

In exploring the reactions between Ti thin films and the Si substrates *in-situ* monitoring techniques are crucial¹¹. Simultaneous use of different analytical techniques allows a better evaluation of changes occurring in the film. In this work we have used an *in-situ* experimental setup, which combines x-ray diffraction (XRD), resistance measurement and light scattering.

The measurements reported here were performed at beamline X-20C of the National Synchrotron Light Source (NSLS) at Brookhaven National Laboratory. This beamline has been optimized for kinetics studies through the use of a wide-bandpass ($\Delta\lambda/\lambda \approx 1.5\%$) W-Si multilayer monochromator and focusing mirror that

yield a 1x1 mm² spot with a typical flux of 3×10^{13} photons/sec at a ring current of 300 mA and x-ray energy of 6.9 keV (0.1797 nm). In order to monitor the formation of phases in real time, we employed a linear position sensitive detector (PSD). This camera uses a linear diode array of 1024 pixels, giving photon-counting capability with sub-second time resolution. During the phase transformations diffraction patterns were collected every 0.5 s. The angular position of the detector (approximately 40-54° 2θ) was chosen so that diffraction peaks from both C49 to C54 phases could be simultaneously measured. Samples were annealed in a high vacuum x-ray furnace employing a graphite/pyrolytic boron nitride heater. All results reported here were performed in a helium atmosphere to promote temperature uniformity and inhibit oxide or nitride formation. The helium gas, which was initially five 9's grade, was passed through a titanium gettering furnace before flowing into the sample chamber. An oxygen monitor on the output helium flow verified that the oxygen content remained below the parts-per-trillion (ppt) level throughout each annealing experiment.

Simultaneous measurements of roughness were made with optical scattering, using 633 nm light, at an incident angle of 65° and scattered angles of -20° and 52° (with two detectors) providing information on length scales of approximately 0.5 μm and 5 μm, respectively. The electrical resistance was measured using a spring loaded four point probe in a square geometry that also holds the sample in place during rotations of the annealing chamber (changing incident x-ray angle θ). The samples were usually squares cut from Si wafers with dimensions of approximately 1.5 cm on the side. The temperature measurements were calibrated using metal silicon eutectics and are precise to ±3 °C.

In addition to the *in-situ* studies of the transformation kinetics, *ex-situ* pole-figure measurements were performed to more completely characterize the sample texture. Pole figures map out the scattered intensity from a particular Bragg reflection as a function of tilt angle away from the sample normal and rotation angle around the sample normal. Thus they indicate the pre-

ferred orientation directions of particular atomic planes in a film. Because of the four-fold rotational symmetry of the silicon substrate lattice, data was collected in only one quarter of the hemisphere.

Sputtered samples were grown on lightly boron-doped Si(001) wafers and undoped poly-Si substrates. Ta and Ti films were deposited consecutively without breaking the vacuum. The thickness of Ti was kept constant at ~27 nm and the interposed Ta layer thickness was varied between 0 and 1.5 nm. Rutherford back-scattering measurements showed approximately 10% oxygen contamination in all as-deposited samples. It is our experience that this is typical in sputtered Ti films of these thicknesses.

In-situ results of a Ti film on poly-Si, without a Ta layer are shown in Figure 1. The sample is annealed at 3 °C/s to 1000 °C in He. The upper panel shows the resistance measurement and the light scattering signals as a function of temperature. The XRD data is shown in the lower panel. The contours and color indicate the intensity of the diffracted x-rays, with blue as low intensity and red as high intensity. XRD spectra start with the Ti peaks of (002) and (101) reflections.

These peaks, especially (002), shift to higher angles due to Ti reaction with oxygen¹². The light scattering signals are featureless until the C49 phase formation. As the (131) diffraction line of C49 phase appears, the resistance curve shows a sharp drop and the 0.5 μm scale light scattering signal increases, indicating film roughening. The 5 μm scale signal has a maximum at this time. A significant increase in the 5 μm length scale roughness seems suspicious during a phase formation that is a few tens of nanometers thick. However unlike the 0.5 μm length scale the 5 μm scale signal is mostly sensitive to the lateral uniformities, such as an index of refraction change, which occur when a new phase nucleates. Therefore, the signal reaches a maximum where non-uniformity is highest and returns to its original value when the film becomes laterally homogeneous again (complete transformation into a new phase). Along with the C49 (131) peak, two weak peaks are seen at ~50.5° and 49.5°, which can be assigned to Ti_5Si_4 (302) or (311) and Ti_5Si_3 (300), respectively. The C54 phase starts to form after 800 °C, with (311) orientation. The resistance drops again and both light scattering signals respond with small changes.

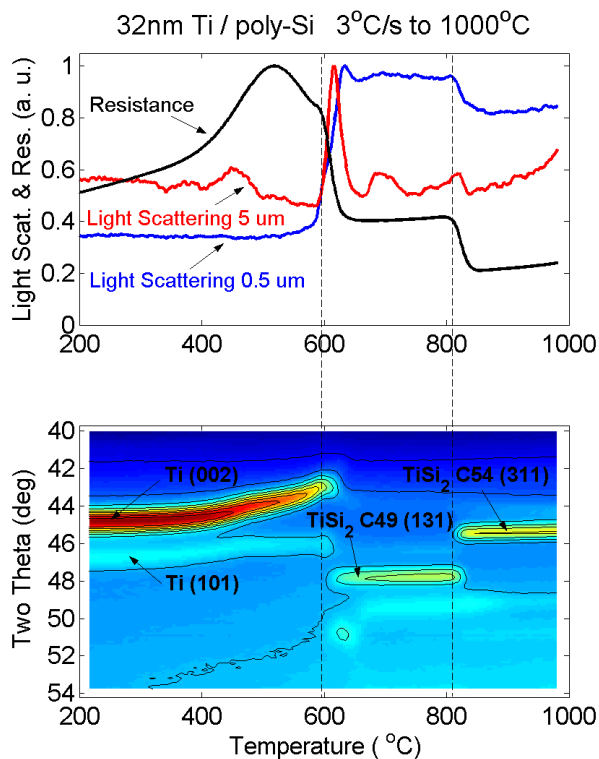


Figure 1. Upper panel: Normalized in-situ resistance and light scattering signals of a 27 nm Ti /poly-Si sample annealed at 1000 °C with 3 °C/s in He. Lower panel: Contour plot of the in-situ XRD result. The vertical axis represents the diffraction angle (2θ).

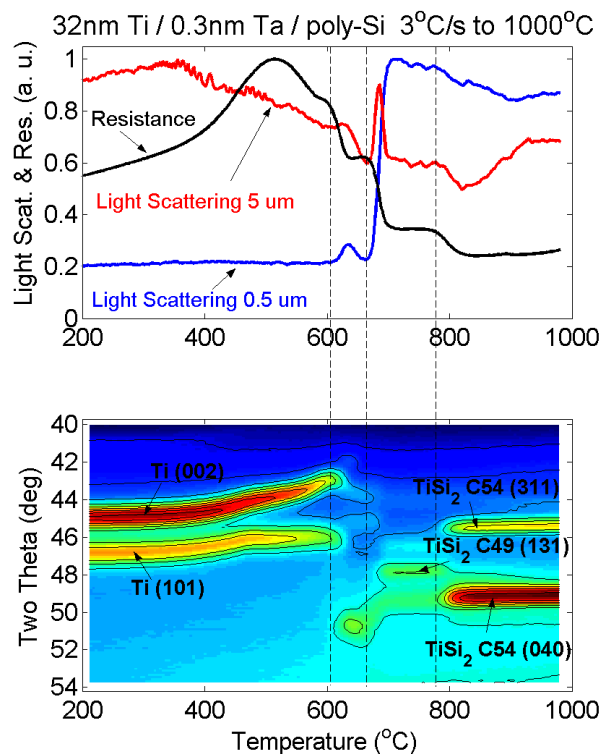


Figure 2. Upper panel: Normalized in-situ resistance and light scattering signals of a 27 nm Ti /0.3 nm /poly-Si sample annealed at 1000 °C with 3 °C/s in He. Lower panel: Contour plot of the in-situ XRD result. The vertical axis represents the diffraction angle (2θ).

When a 0.3 nm Ta layer is interposed between Ti and the poly-Si substrate, the kinetics and texture of the phases are significantly different (Figure 2). C49 phase formation is delayed approximately 100 °C and the metal-rich peaks are more intense. The delay of C49 phase growth is also observed by the light scattering signals. Note that the resistance curve has an extra step, which does not exist for the pure Ti film. The decrease in resistance at 600 °C indicates the metal-rich phase formation and the second drop is due to the C49 phase formation. For this Ta thickness, the C54 phase forms at a lower temperature (~780 °C) and its texture is dominantly (040) instead of (311).

These results are similar to those we found for a film with Ta interlayer on Si(001) substrate. In order to investigate the relationship of the C54 phase to the substrate we have performed pole figure analysis on a 0.3 nm Ta film on Si(001) in C54 phase. The results (Figure 3) confirm the presence of a strong (040) texture normal to the film plane. A weak in-plane texture is also seen. In particular the (022) poles are not randomly distributed in a ring at 56° (the angle between (040) and (022)) away from the normal direction but there is more intensity along directions that project down onto the Si <110> directions (the axes of the pole figure).

Tantalum interlayers thinner than 0.3 nm were not very effective for the enhancement of C54 phase. Ta interlayers thicker than 0.3 nm stabilized the metal-rich phases and the (Ti,Ta)Si₂ C40 phase, causing a delay in the C54 phase formation. These results can be explained by the slow diffusion of Si in the presence of a Ta interlayer since we have seen an increased amount of metal-rich and C40 phases as a function of increasing Ta thickness.

The enhancement and texture evolution of the C54 phase in the case of a 0.3 nm Ta layer can be attributed to a template mechanism provided by the metal-rich Ti₅Si₃ phase rather than the C40 phase. C40 (001) and Ti₅Si₃ (100) planes have good lattice matches with the C54 <010> planes. If the template mechanism of either phase were operative, one would expect to see the <100> diffraction line of the C40 phase or (100) diffraction line of the Ti₅Si₃ phase since the C54 phase forms with a strong (010) orientation. The Ti₅Si₃ phase has a sharp (100) texture, which is also confirmed with *ex-situ* XRD analysis, and it supports a template mechanism acting between the (100) planes of the Ti₅Si₃ phase and the (010) planes of the C54 disilicide phase.

In summary, we have studied the formation of titanium silicides in the presence of an ultra-thin layer of Ta, interposed between Ti and Si. The most effective Ta thickness for lowering the C54 phase formation is 0.3 nm and it fundamentally changes the C54 film texture. The time-resolved XRD shows that the volume

fraction of C40 and metal-rich silicide phases grows with increasing Ta layer thickness. Increased Ta layer thicknesses also cause delayed growth of the C49 disilicide phase.

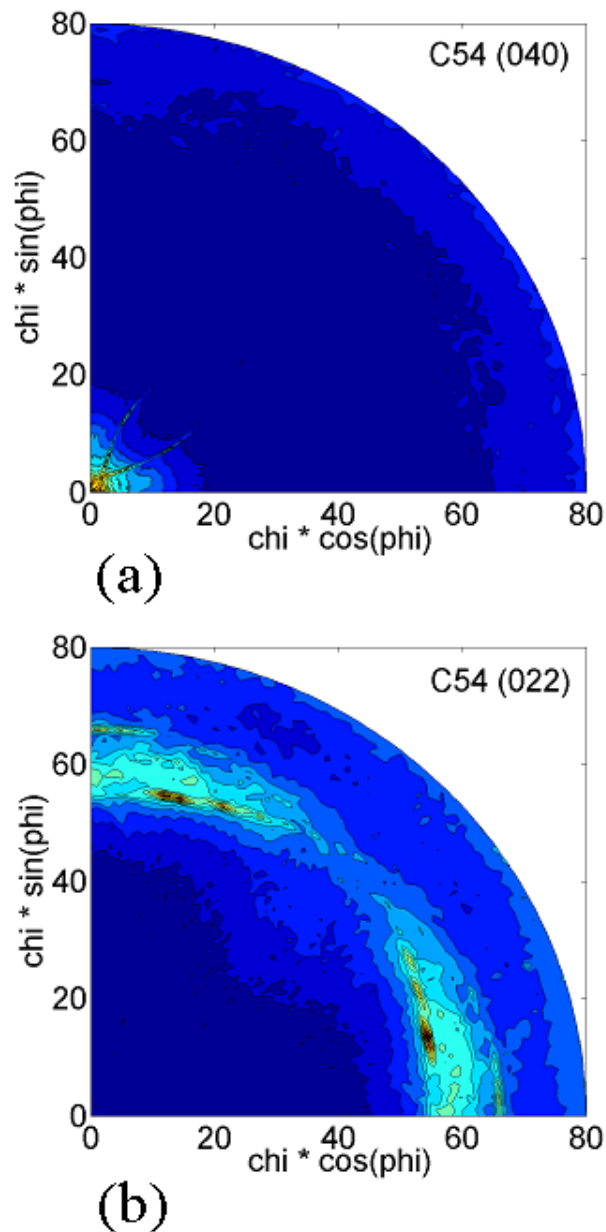


Figure 3. Pole figures of a 27 nm Ti film with 0.3 nm Ta on Si(001) annealed at 1000 °C with 3 °C/s in He. a) C54(040); b) C54(022). The x- and y-axes correspond to the projection directions of the substrate Si $[\bar{1}10]$ and $[110]$ respectively.

Acknowledgements

The authors thank Steve LaMarra for his help with the *in-situ* experiments and Roy Carruthers for sample deposition. This work was partially supported by NSF ECS-9515181. The National Synchrotron Light Source is supported by the U.S. Department of Energy, Division of Materials Science and Division of Chemical Sciences under Contract Number DE-AC02-98CH10886.

References

- [1] Z. Ma and L. H. Allen, Phys. Rev. B **49**, 13501, 1994.
- [2] L. A. Clevenger and R. W. Mann, Mat. Res. Soc. Symp. Proc. **320**, 15, 1994.
- [3] L. A. C. R. A. Roy, C. Cabral, Jr., K.L. Saenger, S. Brauer, J. Jordan-Sweet, G. Morales, K. F. Ludwig, Appl. Phys. Lett. **66**, 1732, 1995.
- [4] A. Mouroux, S. -L. Zhang, W. Kaplan, S. Nygren, M. Ostling and C.S. Petersson, Appl. Phys. Lett. **67**, 975, 1996.
- [5] C. Cabral, Jr., L. A. Clevenger, J. M. E. Harper, F. M. d'Heurle, R. A. Roy, K. L. Saenger, G. L. Miles, R. W. Mann, J. Mat. Sci. **12**, 304, 1997.
- [6] A. Mouroux, S. -L. Zhang and C. S. Petersson, Phys. Rev. B **56**, 10614, 1997.
- [7] A. Mouroux, T. Epicier, S.-L. Zhang, and P. Pinard, Phys. Rev. B **60**, 9165, 1999.
- [8] J. M. E. Harper, J. C. Cabral, and C. Lavoie, Annu. Rev. Mater. Sci. **30**, 523, 2000.
- [9] S. -L. Zhang, F. M. d'Heurle, Appl. Phys Lett. **76**, 1831, 2000.
- [10] S. -L. Zhang, F. M. d'Heurle, C. Lavoie, C. Cabral, Jr., J. M. E. Harper, Appl. Phys. Lett. **73**, 312, 1998.
- [11] C. Lavoie, J. C. Cabral, F. M. d'Heurle, and J. M. E. Harper, Defect and Diffusion Forum 194-199, 2001.
- [12] R. Cocchi, D. Giubertoni, G. Ottaviani, T. Marangon, G. Mastracchio, G. Queirolo, A. Sabbadini, J. Appl. Phys. **89**, 6079, 2001.